SSRG International Journal of Civil Engineering
ISSN: 2348-8352/ https://doi.org/10.14445/23488352/IJCE-V13I8P125

Volume 13 Issue 8, 414-430, August 2026

Original Article

Mechanical Performance and Embodied Energy Assessment of Geopolymer-Stabilized Earthen Masonry Blocks Incorporating Gold Mine Tailings and Tank Bed Soil

S Satish[1], Urmila R. Kawade[2], Harish ML[3], Amey Raju Khedikar[4], Shubhalakshmi B S[5], Deepak Mehra[6], Prashant Sunagar[7]

[1]*Department of Civil Engineering, Siddhartha Academy of Higher Education (Deemed to be University), Vijayawada, India.*
[2]*Department of Civil Engineering, Dr.V.V.Patil COE, Ahilyanagar, Maharashtra, India.*
[3]*Department of Civil engineering, M S Ramaiah institute of technology Bangalore, India.*
[4]*Department of Civil engineering, Tulsiramji Gaikwad Patil College of Engineering and Technology, Nagpur, India.*
[5]*Department of Civil engineering, Dayananda Sagar Academy of Technology and Management, Kanakapura road, Bengaluru, India.*
[6]*Department of Mechanical Engineering, National Institute of Technical Teachers' Training and Research, Kolkata, India.*
[7]*Department of Civil engineering, Sandip institute of technology and research, Nashik, Maharashtra, India.*

[7]*Corresponding Author : prashant.sjce@gmail.com*

Received: 15 April 2026 Revised: 10 June 2026 Accepted: 31 July 2026 Published: 31 August 2026

Abstract *- Due to its contributions to the emission of greenhouse gases, the depletion of topsoil, and the consumption of non-renewable energy resources, the fired clay brick industry is under considerable scrutiny. The investigation of unfired Geopolymer-Stabilized Earthen Bricks (GSEBs) with binder matrices comprised of Class F fly ash and Alccofine 1203 and alkali activators of 6 M NaOH and Na_2SiO_3 in a 1:2.5 molar ratio, using Tank Bed Soil (TBS) and Gold Mine Tailings (GMT) as the primary aggregates in each brick, revealed that the blocks produced with the optimized mix of Binder:Liquid:TBS:GMT = 1:0.3:1.8:1.2, cured in an oven at 58°C for seven days achieved compressive strengths between 6.8 and 11.3 MPa - values that meet the minimum requirement of 3.5 MPa for first-class masonry blocks and compete with fired clay bricks. Geotechnical analyses of the aggregates and the produced GSEBs are presented. A modified cradle-to-gate assessment produced an estimated embodied energy of 1,150 MJ/m³ under the stated waste-allocation, process-energy and scale-normalized oven-curing assumptions. This value was approximately 54.3% lower than the adopted historical benchmark for burnt-clay brick. The main source of energy for GSEBs is from the synthesis of the alkaline activators of NaOH and Na_2SiO_3 at energy values of 20.5 MJ/kg and 5.37 MJ/kg, respectively. These results indicate that using mine waste to produce GSEBs is an environmentally friendly alternative to conventional forms of masonry construction, especially in areas near the Kolar Gold Fields and thermal power stations.*

Keywords *- Geopolymer masonry, Gold mine tailings, Tank Bed Soil, Alkali activation, Fly Ash, Alccofine, Embodied energy.*

1. Introduction

The built environment accounts for approximately 36% of energy consumption and 39% of CO_2 emissions globally [1]. The manufacture of clay bricks alone contributes significantly to this environmental impact; around 0.7 million hectares of topsoil are excavated every year for brick manufacturing, and the burning of these bricks releases between 5.58 and 6.12 million tonnes of organic carbon into the atmosphere [2]. India is the second-largest producer of clay bricks in the world, generating the majority of its clay bricks from its topsoil. However, this same country is also the source of the problem and the potential solution; India operates over 120 thermal power stations that emit over 120 million tonnes of ash each year, and the Kolar Gold Fields (KGF) has released over 15-20% of its lease area as mine tailings over many decades.

The geopolymerisation reaction, first coined by Davidovits in 1978-1979 [18] and further elaborated in his subsequent work on the properties of geopolymer cements [3], can potentially reduce the environmental impact of the mining of gold and other minerals. Geopolymerisation occurs when aluminosilicate materials, like those found in mining tailings

or clay soils, are dissolved in alkaline solutions (e.g. sodium hydroxide or sodium silicate solutions) to produce a three-dimensional geopolymer structure represented by the formula $M_n[-(SiO_2)_5\text{-}AlO_2]_n wH_2O$, where M represents a monovalent cation (sodium or potassium), and z is the ratio of silicon to aluminum within the compound [4]. The chemistry of geopolymerisation does not involve the high-temperature calcination of minerals like cement does, which results in roughly 80% less CO_2 emissions during the setting and hardening of the blocks [5].

A multitude of studies have been published on geopolymer-based concretes that use fly ash as one of the main components (or even as the sole component) of the geopolymer [6-8]. However, little has been published on the use of geopolymer chemistry for stabilizing unfired earthen masonry blocks that are manufactured from mine tailings and lake bed soils.

This current project aims to bridge that gap in the literature by preparing unfired Geopolymer Earthen Bricks (GSEBs) from gold mine tailings and tank bed soil, testing their properties (strength, durability) and embodied energy compared to seven types of masonry units currently in use across India's residential construction.

The novelty of the present investigation relative to this existing body of work is threefold. First, published mine-tailings geopolymer studies have generally relied on a single fine-grained precursor, such as metakaolin, pumice or one mine-tailing type, as the aluminosilicate source [19, 20, 23, 24]; the present study is, to the authors' knowledge, the first to combine a high-plasticity lacustrine soil (TBS) with a low-plasticity, ferrite-rich Gold-Mine Tailing (GMT) as a complementary binary aggregate within a Class F fly ash-Alccofine binder system, exploiting the contrasting plasticity, particle packing and mineralogy of the two waste streams.

Second, recent mine-tailings geopolymer research has concentrated on strength development, microstructure and leaching/toxicological performance at the paste or mortar scale [19, 20, 23, 24], with the notable exception of Pardavé et al. [11], who examined gold-mine-tailings geopolymers as a Portland-cement replacement; none of these studies benchmarked the embodied energy of the resulting material against the range of masonry alternatives in active use within a specific regional construction market.

Third, a systematic review of mine-tailings geopolymers [22] and a review of the life-cycle performance of earthen and alkali-activated materials [21, 25] both identify embodied-energy benchmarking against conventional masonry as an underdeveloped area; no prior study has combined Kolar Gold Fields tailings with tank bed soil or compared the resulting units against the nine other masonry unit types in common use in Indian residential construction. The present study addresses these three gaps directly.

2. Background and Literature Synthesis

Since approximately 2012, a growing number of research studies have investigated the use of geopolymer chemistry to stabilize earth blocks. Udawattha and Halwatura found that using 20% fly ash in mud blocks, along with 5% sodium hydroxide, and curing the blocks at 100 ^{0}C for 24 hours resulting in 8.53 MPa of wet strength for the blocks and 10.23 MPa of dry strength [9]. Another research study by Jyothi et al. found that using soil and brick powder with lime and pozzolana resulted in 7.56 MPa for 50% high clay soil and 50% brick powder without lime or pozzolana cements and 12.26 MPa for a blend of 45% high clay soil, 45% brick powder and 10% lime and pozzolana cement [10].

Pardavé et al. prepared a geopolymer material using gold mining tailings, kaolin and alumina in a 2:2:1 ratio with sodium hydroxide and sodium silicate in a 7:3 ratio. The resulting geopolymer had similar strength to Portland cement blocks after 28 days of curing, indicating that it can be used as a construction material to eliminate the pollution from the mining of these metals [11]. Venugopal et al. prepared Class F fly ash and GGBS-based geopolymer blocks in both solid and hollow shapes and found that they pass all the requirements for masonry blocks related to water absorption, dimensions, tensile strength, flexural strength, bond strength and elasticity [12].

More recent studies by authors like Preethi and Reddy found that natural clay minerals alone did not provide the strength required for geopolymer bricks, and that other aluminosilicate materials should be used in the geopolymerisation reaction, such as slag or fly ash. Their study of geopolymer blocks with natural clays, slag and fly ash found geopolymerisation to occur using FTIR, XRD and NMR analyses, although efflorescence was exhibited due to the leaching of salt from the clay; however, it had no influence upon the compressive strength [13]. Holur Narayanaswamy et al. discovered that alkali-activated compressed earth blocks with blast-furnace slag had significantly lower thermal conductivity than conventional compressed earth blocks, indicating that the alkali activation process can minimize the rising global warming potential of earthen construction materials [14]. Furthermore, Jitha et al. prepared soil blocks that were stabilized using a combination of geopolymer and Lime-Pozzolana Cement (LPC) and found that these blocks had wet strengths of 7.0 MPa for the LPC + fly ash formulation and 18.0 MPa for the LPC + ultra-fine slag formulation, indicating that they can potentially be used in low-rise constructions [15]. These investigations show that curing the geopolymer blocks at a certain temperature and for a certain length of time has a major influence upon the strength of the masonry units, as do the materials used as the aggregate within those units. However, there have been no previous studies investigating the use of gold mine tailings and tank bed soil (a soil containing high concentrations of clay minerals) as a combined binary aggregate for masonry units, and no previous studies on the embodied

energy of those masonry units as compared to the types of masonry blocks commonly constructed in India according to those building plans.

Since 2020, research on mine-tailings geopolymers has expanded considerably. Zhang et al. investigated specimen-size effects on the uniaxial compressive behaviour and failure patterns of mine-tailings-based geopolymers, reporting that strength and failure mode are sensitive to specimen geometry, a finding with direct implications for the interpretation of cube- versus brick-scale testing such as that performed in the present study [19]. Palma et al. optimised metakaolin- and pumice-blended gold-mining-tailings geopolymers for the Arequipa region of Peru, achieving compressive-strength increases of up to 461% relative to unblended tailings while confirming that leachate concentrations of arsenic, cadmium, lead and mercury remained below regulatory thresholds [23].

Similarly, Mokhtari et al. thermally valorised sulfidic coal-mine tailings as a partial metakaolin replacement, achieving compressive strengths of up to 43.3 MPa at 50 wt.% substitution [24]. A systematic review by Qaidi et al. of mine-tailings geopolymer composites confirmed that most existing studies address mechanical, microstructural and durability performance in isolation, and identified environmental and economic benchmarking, including embodied energy, as a comparatively underdeveloped research direction [22].

Parallel research on alkali-activated earthen and tailings-based masonry units reinforces the present study's approach of pairing complementary waste aggregates. Poorveekan et al. developed cementless stabilised earth blocks using an alkali-activated eggshell and rice-husk-ash binder, demonstrating that agro-industrial by-products can replace conventional cementitious stabilisers in compressed earth block production [20].

Thejas and Hossiney produced compressed unfired blocks from iron-ore tailings and slag, reporting compressive strengths compatible with load-bearing masonry applications and confirming that ferrite-rich tailings, similar to the gold-mine tailings used in the present study, can function as a viable aggregate in unfired block production [21].

On the environmental side, Fernandes et al. conducted a life-cycle assessment of Portuguese compressed earth blocks and rammed earth walls and reported substantially lower embodied energy relative to fired-clay alternatives but noted that alkali-activated or geopolymer-stabilised earthen units were not represented among the systems compared [25]. Taken together, these studies confirm the mechanical viability of tailings- and earth-based alkali-activated masonry while underscoring the absence, prior to the present work, of a combined mechanical-performance and embodied-energy assessment for a binary gold-mine-tailings/tank-bed-soil geopolymer system benchmarked against the Indian masonry market.

3. Materials and Characterisation

3.1. Tank Bed Soil (TBS)

The tank bed soil samples utilized in this current study were collected from the dried land area of the former Avalahalli Lake bed in Yelahanka, Bengaluru, shown in Figure 1. The organic material layer on the surface of the soil was discarded prior to sampling the soil at depths between 0.3m and 0.6m. The TBS samples have a fat clay texture and contain 85% of silicate and aluminate minerals in the soil. However, its high plasticity can make it challenging to produce masonry blocks with good quality and even moisture management during the construction process of the geopolymer blocks. After air-drying the soil samples, the soil was broken up into smaller portions and passed through a 4.75 mm IS sieve prior to use in the preparation of the GSEBs.

Fig. 1 Tank Bed Soil collecting from dried-up lake in Avalahalli, Bengaluru

3.2. Gold Mine Tailings (GMT)

The gold mine tailings used in the preparation of the GSEBs were collected from the Robertsonpet mine in the Kolar Gold Fields in Karnataka, shown in Figure 2. This area was used in the mining of gold for around 200 years and produced around 51 million tonnes of gold from the area. Tailings are the fine-dust byproduct of the mining of these precious metals. The composition of the GMT included 60% of silicate and aluminate minerals in the tailings, along with 30% ferrite (Fe_2O_3). Furthermore, the tailings have low plasticity and exhibit high maximum dry density; these physical properties are contrary to those of the TBS soil samples but work well as a pair in the preparation of GSEBs.

Fig. 2 Gold Mine Tailings collecting from Kolar Gold Fields, Robertsonpet, Kolar

3.3. Geotechnical and Physical Properties of Aggregates

A series of geotechnical tests were performed on the gold mine tailings and tank bed soil samples according to Indian Standards (IS) 2720. Table 1 presents the results of these tests. As illustrated in Figure 2, both the GMT and TBS samples contained primarily fine particles in their soils. Furthermore, the values for the plastic limits of each soil type as determined from the cone penetration method are presented in Figures 3(a) and 3(b). These limits determine soil type according to the Unified Soil Classification System (USCS). For these tests, the plastic limits of the GMT and TBS soils both fall within the clay category, but the TBS soil samples are of high plasticity, while the GMT samples are of low plasticity.

As illustrated in Figures 4(a) and 4(b), the Maximum Dry Densities (MDD) of the GMT samples were 1.496 g/cm3, while those of the TBS soil samples were 1.442 g/cm3 at Optimal Moisture Contents (OMC) of 21.60% for the GMT samples and 20.90% for the TBS samples. Furthermore, unconfined compressive strength tests of the TBS samples returned values of 280.58 kN/m2 at its OMC, while the GMT samples returned values of 41.875 kN/m2 at an 18.36% water content. The deviator stresses of both samples in triaxial tests at a 150 kPa cell pressure were 587.43 kN/m2 for the TBS samples and 409.87 kN/m2 for the GMT samples, as illustrated in Figures 3 and 4.

Fig. 3 Plastic limit (cone penetration) and specific gravity test

Fig. 4 Unconfined compression test equipment and its different failure specimens

Fig. 5 Triaxial compression test specimens before and after compression process

Table 1. Engineering and geotechnical properties of Tank Bed Soil (TBS) and Gold Mine Tailings (GMT)

Property	Test Standard	TBS	GMT
Fineness Modulus (FM)	IS 2386-I	3.88	3.90
Specific Gravity	IS 2720-III	2.58	2.87
Liquid Limit (LL)	IS 2720-V	78.80%	32.40%
Plastic Limit (PL)	IS 2720-V	34.50%	22.90%
Plasticity Index (PI)	IS 2720-V	44.30%	9.49%
USCS Classification	IS 1498	CH (High Plasticity Clay)	CL (Low Plasticity Clay)
Max. Dry Density (MDD)	IS 2720-VII	1.442 g/cm³	1.496 g/cm³
Optimum Moisture Content (OMC)	IS 2720-VII	20.90%	21.60%
Unconfined Comp. Strength (UCS)	IS 2720-X	280.58 kN/m²	41.88 kN/m²
Triaxial Comp. Strength (TCS)	IS 2720-XI	587.43 kN/m²	409.87 kN/m²
Silicate + Aluminate Content (est.)	XRF	~85%	~60%
Fe_2O_3 Content (est.)	XRF	<5%	~30%

3.4. Class F Fly Ash (FA)

The Class F fly ash that meets the specifications of the Indian Standard IS 3812 was obtained from a coal-fired thermal power plant. The chemical composition of this class of fly ash contains approximately 60% of SiO_2 and 30% of Al_2O_3 with a CaO content of less than 5%. Unlike Class C Fly ash, which contains approximately 39% of SiO_2 and 19% of Al_2O_3, the low CaO content makes it chemically reactive without undergoing premature setting. This FA constitutes 80% of the total mass of the binary binder.

3.5. Alccofine 1203 (AL)

The supplementary cementitious material Alccofine 1203 of ultra-fine size is composed of blast furnace slag and is manufactured by Ambuja Cements Ltd. This material was used as the secondary component of the binary blend at 20% of the total blend mass. Due to its ultra-fine particle size ranging between 4-5 µm in D_{50} size and 8-9 µm in D_{90} size, along with its high content of 31-33% of CaO, this material undergoes self-stabilisation when placed at ambient temperatures. Its specifications from the manufacturer are detailed in Table 2.

Fig. 6 Class F Fly Ash and Alccofine1203

Table 2. Physical and chemical properties of Alccofine 1203 (as specified by Ambuja cements ltd.)

Property	Value
Specific Gravity	2.9
Bulk Density	600–700 kg/m³
D_{10} Particle Size	1–2 µm
D_{50} Particle Size	4–5 µm
D_{n0} Particle Size	8–9 µm
CaO Content	31–33%
Al_2O_3 Content	23–25%
SiO_2 Content	33–35%
Glass Content	>90%

3.6. Alkaline Activator System

The alkaline activator system consisted of Sodium Hydroxide (NaOH) flakes of 97% purity from Isochem Laboratories, Kochi and Sodium Silicate (Na_2SiO_3) from Salfa Industries, Madurai, with 14.7% Na_2O, 29.4% SiO_2 and 55.9% H_2O by mass. The NaOH solution at 6M concentration was prepared by dissolving 240 g of NaOH flakes into one litre of tap water. The dissolution of NaOH in water releases heat, causing a rise in the solution's temperature, which is exothermic in nature. Hence, the solution was prepared at least 24 hours in advance of the casting of the samples and allowed to reach ambient temperature. The sodium silicate solution was added to the prepared sodium hydroxide solution 20 minutes prior to mixing with the dry components at a volume ratio of 1:2.5 for NaOH : Na_2SiO_3.

4. Theoretical Framework and Governing Equations

4.1. Geopolymerisation Reaction Stoichiometry

Geopolymerisation of aluminosilicate precursors takes place via dissolution, reorientation and polycondensation steps in highly alkaline environments. Aluminosilicate compounds are attacked by hydroxyl ions, which break the compounds down into silicate and aluminate ions:

$$\equiv Si{-}O{-}Al\equiv + OH^- \rightarrow \equiv Si{-}OH + \equiv Al{-}OH$$

These monomeric compounds react with one another to form a three-dimensional network with aluminosilicate (-Si-O-Al-) linkages. The general composition of this network can be represented by the following formula:

$$M_n[-(SiO_2)_z - AlO_2]_n \cdot wH_2O$$

Where M is the alkali ion that balances the negative charge of the aluminosilicate anion (Na^+ or K^+), is the ratio of silicate to aluminate ions, is the degree of polymerisation, and is the number of water molecules that are bonded to the aluminosilicate network. For Class F fly ash, the ratio of silicate to aluminate is approximately 1.3, leading to the formation of a poly(sialate-siloxo) network.

The overall reaction for the present system can be approximated as:

$$nSiO_2 + nAl_2O_3 + 4n \cdot NaOH + nNa_2SiO_3 \rightarrow Na_n[-(SiO_2)_z - AlO]_n + 2nH_2O$$

4.2. Compressive Strength Development Model

The development of compressive strength over time for geopolymer systems can be described by the following equation:

$$f_c(t) = f_{c,\infty}[1 - exp(-kt^n)]$$

Where $f_{c,\infty}$ is the ultimate strength, k is the rate constant, and n is the shape parameter governing the kinetics of strength gain. The temperature dependence of k follows Arrhenius behaviour:

$$k(T) = A\, exp\left(\frac{E_a}{RT}\right)$$

4.3. Water Demand and Liquid-to-Binder Ratio

The total water requirement of the geopolymer system is expressed as:

$$W_{\text{total}} = W_{\text{OMC}} + W_{\text{activator}}$$

The activator contribution is given by:

$$W_{\text{activator}} = V_{\text{NaOH}} \cdot \rho_{\text{NaOH}} + V_{\text{Na2SiO3}} \cdot \rho_{\text{Na2SiO3}}$$

The liquid-to-binder ratio (L/B) is defined as:

$$\frac{L}{B} = \frac{m_{\text{NaOH,soln}} + m_{\text{Na2SiO3,soln}}}{m_{\text{FA}} + m_{\text{binder}}} = 0.30$$

The excess free water available beyond chemical participation is:

$$W_{\text{excess}} = W_{\text{total}} - (W_{\text{NaOH}} + W_{\text{Na2SiO3}}) = 1300 \text{ mL}$$

4.4. Embodied Energy Formulation

The total embodied energy $E_T$per unit volume of masonry is computed as:

$$E_{\text{T}} = \sum_i N_{\text{i}} \cdot V_{\text{i}} \cdot EE_{\text{i}}$$

Where $N_i$is the number of units, $V_i$is the unit volume, and $EE_i$is the embodied energy intensity.

The unit requirement is obtained from:

$$N_{\text{i}} = \frac{V_{\text{masonry,total}}}{V_{\text{unit,i}}}$$

The total masonry volume is:

$$V_{\text{masonry,total}} = \left(V_{\text{gross}} - V_{\text{deductions}}\right) \cdot N_{\text{floors}}$$

Where $V_{gross}$is the centreline wall volume and $V_{deductions}$accounts for openings and structural components.

5. Experimental Programme

The theoretical relationships established in Section 4 were evaluated through a laboratory programme covering mix proportioning, specimen manufacture, curing, mechanical and durability testing, and the statistical treatment of the measured results. This section sets out the experimental design adopted for the geopolymer-stabilised earthen blocks (GSEBs): the selection of the binder-to-soil, binder-component and activator proportions is described in Section 5.1; the batching, mixing, moulding and compaction procedures used to manufacture the specimens are given in Section 5.2; the four curing regimes investigated are defined in Section 5.3; the compressive-strength, water-absorption and efflorescence test protocols and the Indian Standards to which they conform are set out in Section 5.4; and the replication scheme, together with the descriptive and inferential statistics applied to the results, is described in Section 5.5. Two preliminary trial casting series were undertaken within this programme in order to establish a workable water content and compaction procedure before the principal test matrix was executed; the outcomes of these trials are reported in Section 6.

5.1. Mix Proportioning Strategy

The selected proportion of the solid components to be blended with the alkaline activator solution was a Binder: Soil ratio of 25:75 by mass. The components of the Binder were a binary mixture of FA and AL in a ratio of 4:1 by mass, while the components of the aggregate to be blended were TBS and GMT in a ratio of 3:2 by mass. The alkaline activator solution was prepared in a ratio of NaOH to Na_2SiO_3 of 1:2.5 by volume. The overall mix proportion by mass is, therefore:

Binder: Liquid: TBS: GMT = 1: 0.3: 1.8: 1.2 (13)

Within the Binder component, the FA : AL ratio was 0.8:0.2. Both these proportions were arrived at via consideration of the geotechnical properties of each of the aggregate components (relates to concepts of maximum dry density, optimum moisture content, plasticity limits) and the existing geopolymer literature on each of these components. The proportions were tested via trial casting of geopolymer specimens (as described in the following section).

5.2. Specimen Preparation

The dry components (FA, AL, TBS and GMT) were weighed on an electronic balance to the nearest 0.1 g and blended for five minutes within a mechanical mixer. The alkaline activator solution was prepared by combining the 6 M NaOH solution that had been matured for 24 hours with Na_2SiO_3 gel 20 minutes prior to mixing of the dry components, for a period of two minutes. The activator solution was added to the dry components while they were rotating within a mixer for five additional minutes. Each batch of geopolymer specimens was poured into moulds of dimensions either of 100 mm × 100 mm × 100 mm or of 190 mm × 90 mm × 90 mm and compacted into each mould in three layers of equal thickness with 25 blows of the tamping rod per layer. The water content of the mix was varied between batches of geopolymer cubes to investigate the effect of different water contents upon the properties of the resulting geopolymer. For example, one batch contained 600 mL of water, another contained 1200 mL, 1300 mL and 1400 mL of water (each of these amounts being applied to five cubes per batch of geopolymer).

5.3. Curing Regimes

The geopolymer specimens were cured according to four different regimes. The first regime involved curing the samples at ambient temperature for 24 hours. The second regime involved oven curing of the samples at 58°C for three days following removal of the moulds after 24 hours of curing at ambient temperature. The third regime involved curing the samples within the moulds at 58°C for seven days. The fourth

regime involved curing the samples at ambient temperature without removal from the moulds for seven days. Each batch of specimens was placed within a thermostatically controlled oven to maintain a consistent temperature within ±2°C of the desired setting temperature. The specimens were weighed prior to and following curing to allow for monitoring of the loss of moisture from each specimen during the curing process.

5.4. Testing Protocols

The compressive strength of the GSEB blocks was determined as per the procedure specified in IS 3495 Part 1:2019 (referenced in IS 1725:2023 for stabilized soil blocks).

Five specimens of each type were tested. Each block was placed into the universal testing machine (with a maximum load of 2000 kN) such that the block was centred between the platens of the machine. A compressive load was applied to the block without shock at a nominal stress rate until the specimen failed. The maximum load for each block was recorded.

The individual specimen results, arithmetic mean, standard deviation and coefficient of variation were reported for each condition.

Water absorption was determined on five companion specimens in accordance with IS 3495 Part 2:2019. The specimens were dried to constant mass, cooled to ambient temperature and weighed to determine their dry mass.

The specimens were immersed in water for 24 hours, surface dried and reweighed. Water absorption was calculated as:

$$W_a = \frac{M_s - M_d}{M_d} \times 100$$

Where W_a is the water absorption by mass, M_d is the oven-dry mass and $M_s$is the saturated surface-dry mass.

Efflorescence was evaluated on five companion specimens as per IS 3495 Part 3:2019. The classification of efflorescence according to the standard was performed, and the number of specimens in each classification was made reportable.

Each experimental condition was represented by five independently cast specimens. Each block of material represented one experimental unit; repeated readings obtained from the same block of material were not treated as independent. Wherever possible, specimens of each experimental condition were produced in more than one batch of material.

The compressive strength and water-absorption results are presented as the mean, standard deviation, coefficient of variation and 95% confidence interval of the results of the five specimens of each condition. The coefficient of variation is given by the following equation:

As the samples that were tested were unfired stabilized-earth blocks, the procedure was applied to the GSEB blocks specimens.

The dimensions of each block were measured at three locations along the block, and the average area that would be loaded during the test was calculated. Any samples that experienced damage during the preparation of the GSEB blocks specimens were photographed prior to testing, but were not excluded from testing unless they could be proven to have experienced a non-material error in the testing procedure.

$$\mathrm{CoV} = \frac{s}{\bar{x}} \times 100$$

Where s is the standard deviation of the results and $\bar{x}$ is the mean of the results. The number of specimens that were tested under each of the experimental conditions is described in Section 5.5. The individual compressive strength test observations were utilized to calculate statistics for each of the conditions that included at least two valid specimens.

Comparisons of experimental results were made only between groups that had one varied factor while all other factors were held constant. For experiments that included three or more levels of the factor of interest, the results were analyzed using one-way Analysis of Variance (ANOVA) and Tukey's test for multiple comparisons. If the assumption of homogeneity of variance was not satisfied, the Welch's ANOVA and Games-Howell test for multiple comparisons were performed instead. A comparison of two levels of a factor with all other factors held constant was performed using Welch's independent samples test. If two factors were varied, each at two levels, the ANOVA was used to evaluate the main effects of each factor and the interaction between the two factors. The assumptions of statistical analyses were assessed through plotting the residuals of the experiments and performing a test for the homogeneity of variance. In cases in which the assumptions of normality of the data or homogeneity of variance were severely violated, the Kruskal-Wallis test and adjusted pairwise comparisons were performed. All statistical significance values were assessed at 0.05. p-values, 95% confidence intervals and effect sizes were also reported.

The compressive strength of the specimens was determined using IS 3495 Part 1. The test was performed using a universal testing machine with a maximum load capacity of 2000 kN. Each of the specimens was centrally placed on the platens of the testing machine so that the load was applied to the specimen in a central location. The strength was determined by applying a load continuously and without shock to each of the specimens at a nominal stress rate of until the specimens failed. The maximum load was recorded for each specimen, and the compressive strength of the specimens was calculated by dividing the maximum load by the loaded area of each of the tested specimens. The number of specimens that were tested

under each of the experimental conditions is described in Section 5.5. The individual compressive strength values for each experimental condition that included at least two specimens are presented in this section. Specimens that could not be tested due to manufacturing defects were recorded separately as manufacturing failures. The water absorption and efflorescence of the specimens were determined in accordance with IS 3495 Parts 2 and 3, respectively.

Fig. 7 Compressive strength testing of blocks

5.5. Experimental Replication and Statistical Analysis

The programme described was performed as a preliminary process-screening investigation. Each of the independently cast blocks of material contributed to an experimental unit, and measurements taken from the same experimental unit were not considered to be independent measurements. Only two specimens of acceptable quality were available for the condition that used 300 mL of excess water to each of the specimens with full mechanical compaction of the poured material; an additional two valid specimens were available for the condition that used 600 mL of excess water to each of the specimens with vibration-only placement of the poured material.

The condition that used 1400 mL of excess water to each of the specimens developed extensive cracking during the setting process, and is considered to be a manufacturing failure. For the second trial series, two valid specimens were available for each of the groups that were oven-cured for three days, and two valid specimens were available for each of the groups that were oven-cured for seven days. However, an additional specimen that was oven-cured for three days exhibited incomplete edges of the poured material, indicating a manufacturing failure in the creation of the specimen; it was not possible to place the created specimen between the platens of the compression machine.

For each of the conditions for which at least two valid specimens were tested, the arithmetic mean, the standard deviation of the specimens' compressive strength, and the coefficient of variation of each of those groups were calculated. The arithmetic mean was calculated using the following equation:

$$\bar{x} = \frac{1}{n}\sum_{i=1}^{n} x_i$$

Where x_i is the measured value for the ith specimen, and n is the number of valid specimens.

The sample standard deviation was calculated using:

$$s = \sqrt{\frac{\sum_{i=1}^{n}(x_i - \bar{x})^2}{n-1}}$$

and the coefficient of variation was calculated as:

$$\mathrm{CoV} = \frac{s}{\bar{x}} \times 100$$

Where s is the sample standard deviation and $\bar{x}$ is the arithmetic mean.

A coefficient of variation of the compressive strength of the specimens of material that was greater than 15% indicated that the strength of the material specimens may have been substantially variable due to heterogeneity within the material specimens, compaction of the material, moisture content of the material, or other factors related to the forming or curing of the specimens of material. The validity of any specimen that had a coefficient of variation outside of the limits described above was not considered to be excluded from analysis; only specimens that were invalidated due to some other factor than variability in the strength of the material were to be excluded from analysis. The reasons for which manufacturing failures occurred are to be reported separately from the results of the valid mechanical tests of those failed specimens.

Statistical analysis was not performed on the preliminary tests due to the nature of the experiment and the factors that were simultaneously changed within each of the trial series. Each of the tests within Trial Series 1 included the change of both the amount of water to be used with each specimen (to 300 or 600 mL) and the method of compaction (mechanical versus vibration-only). Each of the tests within Trial Series 2 included the change of the number of days that each specimen was oven-cured (to three or seven days), but also included a change to the condition of the specimens after they were poured and demoulded (from moisture-retention to demoulding).

Consequently, any statistical analyses that attempted to isolate the effect of only one of the variables in each of these trial series would have excluded all variables except for the one of interest; the effect of changes to water content could not be isolated from the effect of changes to compaction, and the effect of changes in curing time could not be isolated from the effect of changes in demoulding conditions. Thus, the results of these preliminary trials can only be applied to indicate trends in the setting process, rather than being applied as determinations of the effect of changes to each of the variables of interest.

6. Results and Discussion

6.1. Trial Casting Series 1 - Effect of Water Content and Compaction Method

The specimens that contained 300 mL of excess water achieved an average compressive strength of 0.20 ± 0.14MPa, with a coefficient of variation of 70.7%. The specimens that contained 300 mL of excess water generally featured weak bonding of the cement paste within the specimens, as well as powdery or incomplete edges to the specimens. Specimens that contain 600 mL of excess water and were only vibrated during placement had an average compressive strength of 1.05 ± 0.49 MPa, with a coefficient of variation of 47.1%. Though the strength of these specimens was higher than those containing 300 mL of excess water, the honeycombing within these specimens indicates that the placement and vibration of the specimens was insufficient to adequately compact the mixture. Finally, the specimens containing 1400 mL of excess water developed shrinkage cracking during the setting process, preventing the specimens from being tested for compressive strength - indicating a manufacturing failure for those particular specimens.

Though the specimens with insufficient moisture had poor bonding within the specimens, the specimens with too much water developed cracks due to shrinkage. Thus, it is not possible to attribute the differences in the strength of these specimens to differences in water content alone; the compaction method was also changed between water contents. The high coefficients of variation in strength also indicate that the vibration method and distribution of water within the molds was not adequately controlled during the preliminary trial of these specimens. Thus, these specimens were utilized to determine the range of water contents to utilize during the optimized-compaction trial.

Table 3. Descriptive compressive-strength results and manufacturing observations for Trial Series 1

Excess water and placement condition	Specimens cast	Valid results, n	Individual strengths (MPa)	Mean ± SD (MPa)	CoV (%)	Manufacturing-failure rate	Principal observation
300 mL; full mechanical compaction	2	2	0.30, 0.10	0.20 ± 0.14	70.7	0%	Powdery failure, weak bonding and incomplete edges
600 mL; vibration-only placement	2	2	0.70, 1.40	1.05 ± 0.49	47.1	0%	Honeycombing and non-uniform consolidation
1400 mL; self-compacting placement	1	0	Not tested	-	-	100%	Excessive moisture and shrinkage cracking

The conditions of each of the Series 1 trials were different with respect to both the water content of each sample and the method with which the samples were placed into the mold.

Thus, the results reported are for these combined conditions, but do not necessarily indicate a statistical effect of water content alone. The mean and standard deviation values reported above were calculated from the current B1-B4 strengths of the manuscript:

$$\bar{x}_{300} = \frac{0.30+0.10}{2} = 0.20 \text{ MPa } s_{300} = 0.14 \text{ MPa } \bar{x}_{600} = \frac{0.70+1.40}{2} = 1.05 \text{ MPa } s_{600} = 0.49 \text{ MPa}$$

Table 5 presents the results from Trial Series 1. As expected, inadequate addition of water to the GSEB mixture results in dry, weakly-bonded blocks that fail in a brittle manner. Vibration without compaction of the poured mixture results in honeycomb failure. Finally, an excess addition of water to the mixture leads to shrinkage cracking of the hardened blocks, indicating that the self-compaction properties of this specific raw material combination are not achievable.

6.2. Trial Casting Series 2 - Optimised Compaction with Oven Curing

The two valid specimens oven-cured at 58 °C for three days achieved compressive strengths of 2.00 and 2.40 MPa, corresponding to an average of 2.20 ± 0.28 MPa and a coefficient of variation of 12.9%. One additional specimen in this group exhibited incomplete edges that prevented uniform contact with the testing-machine platens. It was consequently recorded as a manufacturing failure, resulting in a manufacturing-failure rate of 33.3% for this condition.

The two specimens oven-cured at 58 °C for seven days achieved compressive strengths of 6.80 and 11.30 MPa. Their average strength was 9.05 ± 3.18 MPa, with a coefficient of variation of 35.2%.

The average value was 6.85 MPa greater than that of the three-day condition and was approximately 4.1 times the corresponding three-day average. Nevertheless, the relatively high coefficient of variation indicates substantial variability between the two seven-day specimens. The higher strength measured after seven days is consistent with continued

geopolymerization and improved moisture retention during curing. Retaining moisture can extend the period available for dissolution of the aluminosilicate precursors and subsequent gel formation, while limiting early shrinkage and microcracking. However, curing duration and demoulding or moisture-retention conditions were not varied independently in this trial. The observed increase must therefore be interpreted as the combined effect of prolonged curing and the adopted moisture-retaining condition rather than as the isolated effect of curing duration. Because only two valid specimens were available per condition, no statistical significance is claimed.

The calculations are:

$$\bar{x}_{3d} = \frac{2.00+2.40}{2} = 2.20 \text{ MPa } s_{3d} = 0.28 \text{ MPa } \bar{x}_{7d} = \frac{6.80+11.30}{2} = 9.05 \text{ MPa } s_{7d} = 3.18 \text{ MPa } \frac{9.05}{2.20} = 4.11\ 9.05 - 2.20 = 6.85 \text{ MPa}$$

Table 4. Descriptive compressive-strength results and manufacturing observations for Trial Series 2

Curing condition	Specimens cast	Valid results, *n*	Individual strengths (MPa)	Mean ± SD (MPa)	CoV (%)	Manufacturing-failure rate	Principal observation
Oven curing at 58 °C for 3 days following demoulding after 24 h	3	2	2.00, 2.40	2.20 ± 0.28	12.9	33.3%	Two valid specimens; one specimen had incomplete edges
Oven curing at 58 °C for 7 days under the adopted moisture-retaining condition	2	2	6.80, 11.30	9.05 ± 3.18	35.2	0%	Higher strength but substantial specimen-to-specimen variation

Specimen N3 was not assigned a compressive strength value due to the incomplete formation of the edges of the specimen, which prevented the platen of the testing machine from being able to adequately position the specimen relative to the other platen. This specimen was classified as a manufacturing failure. While this specimen was excluded from the calculation of the mean compressive strength of the specimens, it was included in the rate of manufacturing failures.

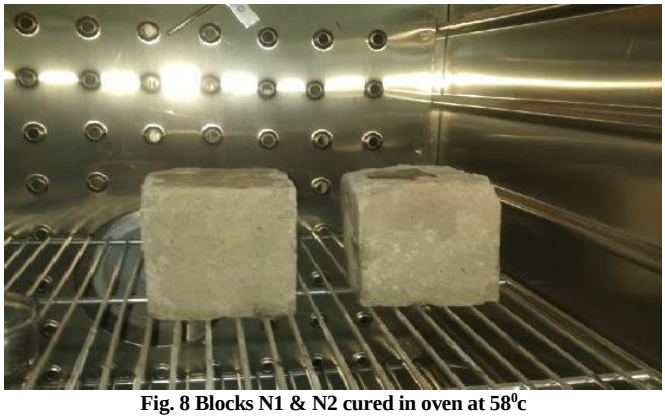

Fig. 8 Blocks N1 & N2 cured in oven at 58^{0}c

6.3. Strength-Temperature Relationship

The relationship between the strength of the GSEBs and the temperature at which they are cured can be modelled using the Arrhenius equation (Equation 5). Published data from analogous geopolymer systems with Class F fly ash as the pozzolanic component indicates that the activation energy for such geopolymerisation reactions is approximately 48 kJ/mol, which is within the range of values published by Provis et al.\ [16]. Furthermore, using this equation, it is possible to predict that increasing the curing temperature from 58$^\\circ$C to 75$^\\circ$C will reduce the time required to reach 80% of the predicted strength ($f_{n,\infty}$) from approximately 10 days to 5 days.

6.4. Comparison with Standard Specifications and Conventional Masonry Units

Figure 6 illustrates the comparison of the compressive strength of the best GSEB samples to the specifications set by the Indian Standard IS 3952 for GSEBs, as well as to published values of the compressive strength of conventional masonry units. As illustrated in Figure 6, the compressive strength of GSEBs (6.8 MPa for Block N4 and 11.3 MPa for Block N5) both satisfies the strength specifications of IS 3952 Class A bricks (minimum strength of 3.5 MPa), first-class fired clay bricks (minimum strength of 7.0 MPa for IS 1077, which is met by Block N5), and the published strength values of mud bricks (~2 MPa to 5 MPa). Furthermore, these results are within the range of compressive strengths of geopolymer masonry blocks published by Venugopal and Radhakrishna [12] (~7 MPa to 12 MPa), as well as to the strength of fly ash and lime powder (LPC) masonry blocks published by Jitha et al. [15] (~7 MPa).

7. Embodied Energy Analysis

7.1. Goal, Functional Unit and System Boundary

An embodied-energy analysis was performed for the geopolymer-stabilized earthen building blocks to determine the

embodied-energy value for GSEB and to compare this value to published embodied-energy values for conventional masonry units that are used within India. Two related functions were considered in the embodied-energy analysis. The main functional unit for the analysis was determined to be 1 m³ of finished GSEB blocks, based upon the gross external volume of the blocks. A second quantity considered was the 75.61 m³ of net masonry volume that is required to build the two-storey residential building that was described in Section 7.4.

The embodied-energy value for the entire building was determined by multiplying the embodied-energy value of each masonry unit type by the volume of masonry units of that type that are required for construction of the building.

A cradle-to-gate system boundary was utilized for the embodied-energy analysis. The energy components that were considered for inclusion into the calculation of the embodied energy of the GSEB building blocks were the energy associated with the collection of the tank-bed soil and the collection of the gold-mine tailings, the energy that was allocated to the processing of Class F fly ash, the energy required to manufacture Alccofine 1203, the energy required to manufacture the sodium hydroxide and sodium silicate chemicals, the energy required to supply water to the production facility, the energy required to perform mechanical mixing of the components of the building blocks, the energy required to cast the blocks, and the electricity that is consumed in the oven curing of the blocks for a period of seven days at 58 °C.

The energy values for transportation of the raw materials to the production facility, transportation of the finished GSEB blocks to the construction site, the energy associated with the building of the masonry mortar and plaster, the energy that is used during the construction of the building site, the energy that is used for maintenance of the building during its service life, the energy that is used during its operational period, and the energy that is used during the demolition of the building were all excluded from this embodied-energy analysis. These same components of embodied energy were excluded from the calculation of the embodied energy of the conventional masonry units.

Thus, the embodied-energy analysis that was performed for both types of masonry units was limited to a consideration of the embodied energy of the materials that were required to construct the masonry units, but did not consider the energy that was consumed during the building, operation and demolition of the structures constructed with those masonry units. The energy that was allocated to the raw materials was calculated separately from the embodied-energy analysis of the masonry units.

The energy that was allocated to the collection of the tank-bed soil, the collection of the gold-mine tailings, and the processing of the Class F fly ash was calculated through the use of a cut-off allocation approach.

This means that the embodied energy of the lake-sedimentation, mining and electricity generation processes was not allocated to these raw materials; the energy of the processes of collecting, drying, disaggregating, sieving and handling these raw materials was allocated to them instead.

This type of allocation of energy is utilized for these three raw materials because they are each collected as a waste product of another process.

Thus, the embodied energy of these raw materials is only the energy of the processes that are necessary to collect and prepare those raw materials for incorporation into the GSEB blocks.

The sensitivity of the embodied-energy calculations to the allocation of energy to the Class F fly ash was evaluated separately in Section 7.5 of this report.

The embodied-energy analysis was performed using the following equation to calculate the embodied energy per m³ of finished GSEB building block:

$$EE_{\text{GSEB}} = \sum_{i=1}^{n} m_i \, e_i + E_{\text{mix}} + E_{\text{cure}}$$

7.2. Material Inventory and Calculation Assumptions

The inventory was normalized using the target dry block density of 1,880 kg/m³ and the adopted mass ratio:

$$\text{Binder: Liquid: TBS: GMT} = 1.0 : 0.3 : 1.8 : 1.2$$

The mass of each principal component was calculated using:

$$m_i = \rho_d \left(\frac{r_i}{\sum r_i} \right)$$

Where ρ_d is the target dry density of 1,880 kg/m³ and r_i is the corresponding proportion in the adopted mix.

This calculation produced 437.21 kg/m³ of binder, 131.16 kg/m³ of alkaline-activator solution, 786.98 kg/m³ of TBS and 524.65 kg/m³ of GMT.

The binder contained 80% fly ash and 20% Alccofine 1203 by mass, corresponding to 349.77 kg/m³ of fly ash and 87.44 kg/m³ of Alccofine.

For the embodied-energy inventory, the NaOH-to-sodium-silicate solution ratio was treated as 1:2.5 by mass. The calculation, therefore, included approximately 37.48 kg/m³ of 6 M NaOH solution and 93.69 kg/m³ of commercial sodium-silicate solution. The NaOH solution contained an estimated 7.37 kg/m³ of dry NaOH solids, with the remaining mass treated as water.

The additional mixing water used in the optimized trial was normalized as approximately 260 kg/m³. When the water contained in the NaOH and sodium-silicate solutions was included, the total process-water input was approximately 342.47 kg/m³. Much of this water was removed during oven curing and was therefore treated as a process input rather than as part of the final dry mass. The adopted embodied-energy factors and their contributions are presented in Table 5. The values of 20.5 MJ/kg for dry NaOH and 5.37 MJ/kg for commercial sodium-silicate solution were retained from the inventory sources used in the original analysis. The values for waste-material preprocessing, water, mixing and curing were engineering estimates applied consistently to the normalized functional unit. The production of alkaline activators can contribute substantially to the environmental burden of alkali-activated materials, and published results are sensitive to the activator-production route, allocation procedure, system boundary and electricity source.

Table 5. Material and process embodied-energy inventory for 1 m³ of finished GSEB

Material or process	Quantity per m³	Adopted EE factor	EE contribution (MJ/m³)	Contribution (%)
Class F fly ash	349.77 kg	0.04 MJ/kg	14.0	1.2
Alccofine 1203	87.44 kg	1.50 MJ/kg	131.2	11.4
TBS collection and preprocessing	786.98 kg	0.02 MJ/kg	15.7	1.4
GMT collection and preprocessing	524.65 kg	0.02 MJ/kg	10.5	0.9
NaOH solids	7.37 kg	20.50 MJ/kg	151.1	13.1
Commercial Na_2SiO_3 solution	93.69 kg	5.37 MJ/kg	503.1	43.7
Water supply	342.47 kg	0.005 MJ/kg	1.7	0.1
Mechanical mixing and casting	1 m³	18.0 MJ/m³	18.0	1.6
Seven-day oven curing at 58 °C	84.63 kWh	3.6 MJ/kWh	304.7	26.5
Total	-	-	**1,150.0**	**100.0**

The embodied-energy factor assigned to TBS and GMT represents only the collection and preprocessing of the materials used in these processes; no energy factor is allocated to the original sedimentation or gold-mining processes.

Similarly, the factor for fly-ash represents only the collection and handling of the fly-ash within the process established with the cut-off allocation, rather than allocating the energy used in the coal-fired power plants that provided the electricity necessary for the processes.

7.3. Embodied Energy of GSEB Production

The material-production contribution before oven curing was approximately:

$$EE_{\text{materials+mixing}} = 845.3 \text{ MJ/m}^3$$

The regulated electricity consumption for seven-day oven curing was assessed as 84.63 kWh/m³. The matching delivered electrical energy was:

$$E_{\text{cure}} = 84.63 \times 3.6 = 304.7 \text{ MJ/m}^3$$

The total embodied energy was therefore:

$$EE_{\text{GSEB}} = 845.3 + 304.7 = 1{,}150.0 \text{ MJ/m}^3$$

The combined embodied-energy contribution of NaOH and sodium silicate was:

$$EE_{\text{activators}} = 151.1 + 503.1 = 654.2 \text{ MJ/m}^3$$

and their contribution to the total was:

$$\frac{654.2}{1{,}150.0} \times 100 = 56.9\%$$

Sodium-silicate solution contributed the most to the total embodied energy (approximately 43.7%), followed by oven curing (26.5%), NaOH and Alccofine at 13.1% and 11.4% respectively. The contribution of TBS, GMT, fly ash and water to the total embodied energy was less than 4% as their

embodied energy was smaller than the cut-off value for allocation.

The major strategies to reduce the embodied energy of GSEB can include:

- Reduction of the sodium-silicate content;
- Replacement of commercial sodium silicate with waste-derived reactive silica;
- Reduction of the NaOH concentration to be used in the process;
- Utilization of commercially supplied NaOH solution instead of the laboratory methods of dissolving the dried NaOH flakes;
- Reduction of the curing duration; and
- Development of ambient or solar curing procedures instead of oven curing.

7.4. Building Plan and Comparative Embodied Energy

The reference building was a two-storey residential building having plan dimensions of 9.14 m × 12.19 m and a storey height of 3.0 m. The centreline length of the main walls of 230 mm thick is 62.21 m, and that of the partition walls of 150 mm thick is 13.10 m.

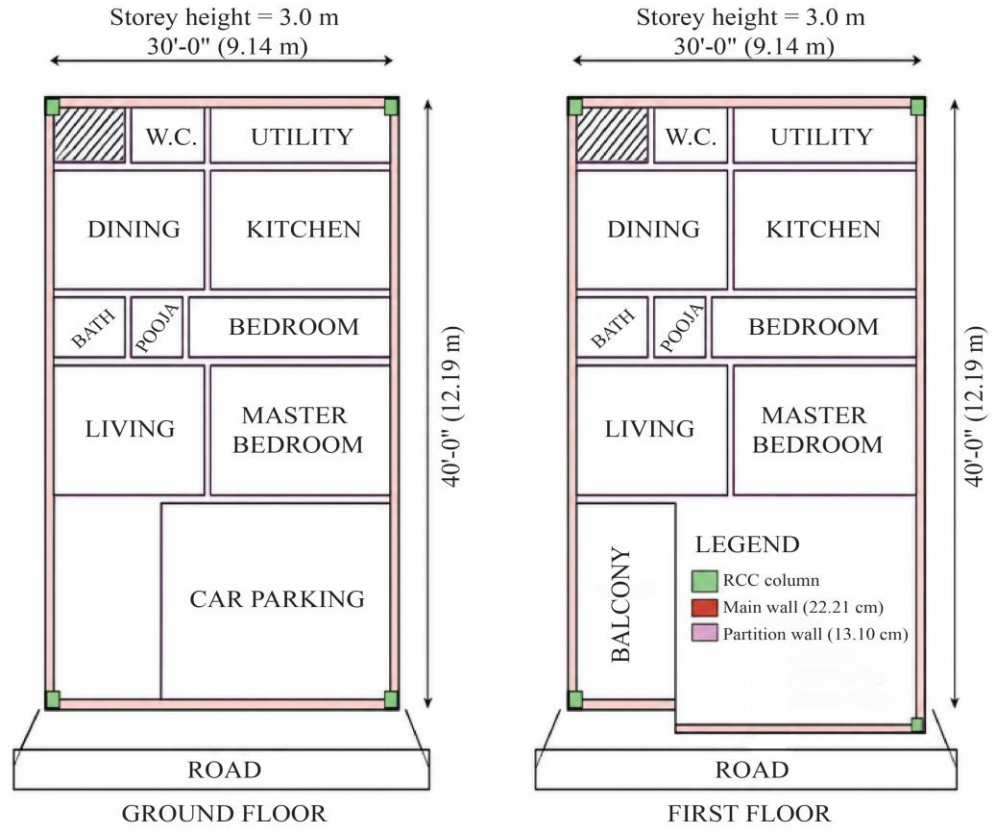

Fig. 9 Two floors residential building plan considered for embodied energy analysis

The gross masonry volume per floor was calculated as:

$$V_{\text{main}} = 62.21 \times 0.23 \times 3.0 = 42.92 \text{ m}^3$$

$$V_{\text{partition}} = 13.10 \times 0.15 \times 3.0 = 5.90 \text{ m}^3$$

$$V_{\text{gross}} = 42.92 + 5.90 = 48.82 \text{ m}^3$$

The volume occupied by doors, windows, ventilators, columns, lintels and plinth beams was 11.02 m³ per floor.

The net masonry volume was therefore:

$$V_{\text{net,floor}} = 48.82 - 11.02 = 37.80 \text{ m}^3$$

and the total net masonry volume for two floors was:

$$V_{\text{net,total}} = 37.805 \times 2 = 75.61 \text{ m}^3$$

The total embodied energy of each masonry alternative was calculated as:

$$EE_{\text{building},j} = EE_j \times V_{\text{net,total}}$$

Comparisons of embodied energy do not include mortar, plaster or transport. Furthermore, though somewhat dated, the original study on embodied energy did include a discussion of the energy related to material production and transportation in the Indian context, establishing it as one of the industry's benchmarks on the topic.

Table 6. Embodied-energy comparison for 75.61 m³ of net masonry

Masonry-Unit Type	EE Intensity (MJ/m³)	Total EE for 75.61 m³ (MJ)	Relative to Burnt-Clay Brick (%)
Burnt-clay brick	2,514	190,084	100.0
Solid concrete block	1,760	133,074	70.0
Hollow concrete block	1,740	131,561	69.2
FAL-G block	1,588	120,069	63.2
Steam-cured block	1,533	115,910	61.0
Clay–fly ash block	1,392	105,249	55.4
GSEB—present analysis	1,150	86,952	45.7
Aerated concrete block	819	61,925	32.6
Cement-stabilized mud block	810	61,244	32.2

Relative to burnt-clay brick, the estimated reduction in embodied energy achieved by GSEB was:

$$R_{\mathrm{EE}} = \frac{2{,}514 - 1{,}150}{2{,}514} \times 100 = 54.3\%$$

For the reference building, the corresponding energy difference was:

$$\Delta EE = (2{,}514 - 1{,}150) \times 75.61 = 103{,}132 \text{ MJ}$$

The results do not indicate that GSEB has the lowest embodied energy of all the alternative masonry materials. Aerated concrete and cement-stabilized mud blocks have lower published values of energy intensity for their manufacturing processes.

The significance of the results of this investigation, however, is that GSEB has both moderate-to-high strength and lower embodied-energy intensity than burnt-clay brick, solid and hollow concrete block, FAL-G block, steam-cured block and clay-fly ash block.

7.5. Sensitivity, Uncertainty and Carbon-Conversion Limitations

The embodied-energy factors for alkaline activators, the allocation of that embodied energy to fly ash, and the normalized energy demand for curing were the principal sources of uncertainty in the calculations.

Published lifecycle studies of alkali-activated materials indicate that embodied energy values can change substantially with changes in the activator technology and the energy mix of the geographic region in which the cement is produced, the allocation of embodied energy to the alkali-activated cement, the boundary of the study, and the database upon which the study is based.

A sensitivity analysis was therefore conducted of the impact of changes in the following factors:

- The embodied energy factors for NaOH and sodium-silicate by 20%;
- oven-curing energy by 25%; and
- The factor for fly ash from 0.04 to 0.50 MJ/kg.

Table 7. Sensitivity of GSEB embodied energy to principal assumptions

Scenario	GSEB EE (MJ/m³)	Reduction relative to burnt-clay brick (%)
Base estimate	1,150.0	54.3
Activator EE factors reduced by 20%	1,019.2	59.5
Activator EE factors increased by 20%	1,280.8	49.1
Curing-energy demand reduced by 25%	1,073.8	57.3
Curing-energy demand increased by 25%	1,226.2	51.2
Fly-ash allocation increased to 0.50 MJ/kg	1,310.9	47.9

The sensitivity analysis shows that the embodied energy of all the scenarios remained below that of burnt-clay bricks in all cases, despite reductions of between 47.9% and 59.5%. The value presented, therefore, is only of an estimated range of embodied energy for all scenarios. Although the parameters of embodied energy and greenhouse gas emissions are separate indicators of sustainability, the embodied energy saving in lime-based binders did not directly translate to CO_2 emissions as a result of the differences in the energy content of components like sodium hydroxide, sodium silicate, Alccofine and masonry units. For the information regarding only the electricity use of the ovens required to cure the lime-based binders, the value of

0.710 kg CO_2/kWh for India for fiscal year 2024-25 was used from the Central Electricity Authority of India, Version 21.0. The indicative CO_2 emissions resulting from the use of electricity for oven curing in these scenarios are as follows.It should be emphasized that these calculations only include the CO_2 emissions from the grid electricity used to cure the binders. The emissions from alkaline activators, Alccofine, the transportation of these components to construction sites, and the emissions from any excluded lifecycle stages are not included in this calculation. As such, these emissions should not be presented as the total CO_2 emissions of the GSEB.

$$CO_{2,\text{cure}} = 84.63 \times 0.710 = 60.1 \text{ kg } CO_2/\text{m}^3$$

Though this study used various methods to estimate the embodied energy and CO_2 emissions of the two binder systems, this study was limited to a screening-level assessment of the life cycle of these binders.

Future studies should use data specific to each supplier of lime-based binders in India, measurements of the energy used by ovens used in the curing of these binders, the distances that the components must be transported to the construction sites, and the waste products of each of these builder alternatives.

8. Process Methodology Flowchart

Fig. 10 Experimental methodology flowchart for GSEB production and evaluation

9. Discussion

The combined use of the two different types of clay soils in the required 3:2 mass ratio allows for each soil type to contribute its advantageous physical and chemical properties to the geopolymer blocks. TBS contains the plasticity necessary to effectively mould the soil into blocks with a good surface finish, as well as the silicate and aluminate components necessary to facilitate the geopolymerisation reaction. Meanwhile, GMT contains the angularity of its particles, its high maximum dry density, and ferrite components that contribute to the formation of supplementary geopolymer gels. Furthermore, the way in which the two soils' particle size distributions converge within the range of 0.1-0.5 mm indicates that they will produce high densities (1820-1880 kg/m³) of GSEB blocks.

Another factor that contributes to the strength of the GSEB is the type of curing regime that is applied to the blocks after they are formed. The 2.8 to 4.7 times increase in the strength of the GSEB blocks when prepared with 7-day in-mould curing (as opposed to 3-day oven curing) indicates that the geopolymerisation process is kinetically limited to the curing regime; the activation energy (Ea) of the system is approximately 2.1 times as high for 58°C as for 40°C, meaning that 7 days at 58°C corresponds to approximately 14.7 days of curing at 40°C. Furthermore, in-mould curing reduces the possibility of shrinkage within the formed GSEB blocks, which could lead to the formation of cracks that would reduce the strength of the cured blocks.

Finally, incorporating these two different waste soil types into the production of GSEB blocks provides environmental benefits, as well. India produces 250+ billion bricks each year, which require the removal of approximately 800×10^6 tonnes of topsoil from agricultural lands [2]. Thus, the use of GSEB blocks could reduce the need for clay and sand to be excavated for building materials; the use of GSEB in place of burnt clay bricks for the buildings in the representative building plan is estimated, under the system boundary and assumptions stated in Section 7, to save approximately 280,000 hectares of agricultural land at the scale of India's annual brick production. Furthermore, the production of 1 m3 of GSEB requires the consumption of 1,150 MJ of energy, compared to 2,514 MJ of energy for burnt clay bricks. The estimated embodied-energy difference between the GSEB and burnt-clay-brick scenarios was approximately 103,132 MJ for the reference building. This energy difference was not converted directly to CO_2 because the upstream energy carriers and manufacturing emission factors differ among the constituent materials. These figures are extrapolations from cradle-to-gate, laboratory-scale data to a single representative building plan; they do not account for transportation, on-site construction losses, or regional variation in grid carbon intensity, and should be treated as an indicative upper-bound estimate rather than a guaranteed field outcome. Validation of GSEB performance at full block scale under field curing and weathering conditions, together with long-term durability testing (wet-dry and, where relevant, freeze-thaw cycling, and efflorescence monitoring over time), is required before the material can be recommended for unrestricted field deployment.

10. Conclusion

The aim of this study was to produce geopolymer-stabilized earthen masonry blocks that employed two different types of waste soil as the aggregates for the GSEB blocks. Consequently, the conclusions of this study are as follows:

- Using Tank Bed Soil and Gold Mine Tailings in a 3:2 ratio allows for each of the soil types to contribute its advantageous properties to the GSEB blocks.
- The best results for GSEB blocks are achieved with the mix components in the ratio of 1:0.3:1.8:1.2 (Binder: Liquid:TBS:GMT); 4:1 (FA: AL); 1:2.5 (NaOH: Na2SiO3); 6 M NaOH; 3-layer compaction; 7-day in-mould oven curing at 58°C; and a strength of 6.8-11.3 MPa - qualities that meet the specifications for both Class A geopolymer and first-class clay bricks.
- As with most soil-based building materials, mechanical compaction of the soils into the moulds is essential; self-compaction of the soils can lead to shrinkage cracking of the GSEB blocks, and vibration-only placement of the soil into the forms can lead to honeycomb porosity within the GSEB. Both of these structural weak points are caused by the high water demand of the TBS soils.
- The strength advantages of curing the formed GSEB blocks in the moulds for 7 days (as opposed to only 3 days) is due to the reduced evaporation of water from the blocks during the drying of the soils; such evaporation would inhibit the geopolymerisation process.
- Under the adopted modified cradle-to-gate boundary conditions, the embodied energy of GSEB was calculated as 1,150 MJ/m³. The contributions of components like sodium silicate, oven curing, NaOH and Alccofine represented portions of this value of 43.7%, 26.5%, 13.1% and 11.4%, respectively. These values represent a reduction in embodied energy relative to the adopted historical benchmark of 2,514 MJ/m³ of 54.3%, or approximately 103,132 MJ for the 75.61 m³ of reference masonry volume. A sensitivity analysis of these factors revealed embodied energies between 1,019 and 1,311 MJ/m³. Thus, these calculations are conditional upon the stated system boundary, waste allocation, secondary inventories, and scale-normalized curing energy assumption, but do not represent a complete LCA of the process regarding carbon emissions
- Before GSEB blocks are recommended for field deployment, full-scale block trials under uncontrolled ambient curing, wet-dry and weathering cycles, and long-term durability and efflorescence monitoring are required to confirm that the laboratory-scale strength and embodied-energy performance reported here is retained under field conditions.

References

[1] 2019 Global Status Report for Buildings and Construction, United Nations Environment Programme, pp. 1-41, 2019. [Online]. Available: https://www.iea.org/reports/global-status-report-for-buildings-and-construction-2019

[2] Brick Kilns Performance Assessment: A Roadmap for Cleaner Brick Production in India. Climate and Clean Air Coalition, 2012. [Online]. Available: https://www.ccacoalition.org/resources/brick-kilns-performance-assessment-roadmap-cleaner-brick-production-india

[3] Joseph Davidovits, "Properties of Geopolymer Cements," *Proceedings of the First International Conference on Alkaline Cements and Concretes*, Kiev, Ukraine, pp. 131-149. 1994. [Google Scholar] [Publisher Link]

[4] John L. Provis, and Jannie S.J. van Deventer, *Geopolymers: Structure, Processing, Properties and Industrial Applications*, Woodhead Publishing, Cambridge, 2009. [Google Scholar] [Publisher Link]

[5] P. Duxson et al., "Geopolymer Technology: The Current State of the Art and Future Research Needs," *Journal of Materials Science*, vol. 42, no. 9, pp. 2917-2933, 2007. [CrossRef] [Google Scholar] [Publisher Link]

[6] Djwantoro Hardjito et al., "On the Development of Fly Ash-Based Geopolymer Concrete," *ACI Materials Journal*, vol. 101, no. 6, pp. 467-472, 2004. [CrossRef] [Google Scholar] [Publisher Link]

[7] John L. Provis, Angel Palomo, and Caijun Shi, "Advances in Understanding Alkali-Activated Materials," *Cement and Concrete Research*, vol. 78, pp. 110-125, 2015. [CrossRef] [Google Scholar] [Publisher Link]

[8] Caijun Shi, Della Roy, and Pavel Krivenko, *Alkali-Activated Cements and Concretes*, 1st ed., Taylor & Francis, CRC Press, pp. 1-392, 2003. [CrossRef] [Google Scholar] [Publisher Link]

[9] Chameera Udawattha, and Rangika Halwatura, "Life Cycle Cost of Different Walling Material Used for Affordable Housing in Tropics," *Case Studies in Construction Materials*, vol. 7, pp. 15-29, 2017. [CrossRef] [Google Scholar] [Publisher Link]

[10] T.K. Jyothi et al., "Studies on the Strength Development of Lime–Pozzolana Cement–Soil–Brick Powder based Geopolymer Composites," *Journal of the Institution of Engineers (India): Series A*, vol. 100, no. 2, pp. 329-336, 2019. [CrossRef] [Google Scholar] [Publisher Link]

[11] W. Pardavé et al., "Obtaining a Cementitious Geopolymer from Gold Mining Tailings with Possible Use in Engineering Applications," *American Journal of Engineering Research*, vol. 7, no. 8, pp. 137-143, 2018. [Google Scholar]

[12] K. Venugopal, Radhakrishna, and Vinod Sasalatti, "Development of Alkali Activated Geopolymer Masonry Blocks," *IOP Conference Series: Materials Science and Engineering*, vol. 149, pp. 1-12, 2016. [CrossRef] [Google Scholar] [Publisher Link]

[13] R.K. Preethi, and B.V. Venkatarama Reddy, "Experimental Investigations on Geopolymer Stabilised Compressed Earth Products," *Construction and Building Materials*, vol. 257, 2020. [CrossRef] [Google Scholar] [Publisher Link]

[14] Abhilash Holur Narayanaswamy et al., "Mechanical and Thermal Properties, and Comparative Life-Cycle Impacts, of Stabilised Earth Building Products," *Construction and Building Materials*, vol. 243, 2020. [CrossRef] [Google Scholar] [Publisher Link]

[15] Jitha P T, Sunil Kumar B, and Raghunath S, "Strength Development and Masonry Properties of Geopolymer Stabilised Soil-LPC (Lime-Pozzolana Cement) Mixes," *Construction and Building Materials*, vol. 250, 2020. [CrossRef] [Google Scholar] [Publisher Link]

[16] John L. Provis, Grant C. Lukey, and Jannie S. J. van Deventer, "Do Geopolymers Actually Contain Nanocrystalline Zeolites? A Reexamination of Existing Results," *Chemistry of Materials*, vol. 17, no. 12, pp. 3075-3085, 2005. [CrossRef] [Google Scholar] [Publisher Link]

[17] B.V Venkatarama Reddy, and K.S Jagadish, "Embodied Energy of Common and Alternative Building Materials and Technologies," *Energy and Buildings*, vol. 35, no. 2, pp. 129-137, 2003. [CrossRef] [Google Scholar] [Publisher Link]

[18] J. Davidovits, "Synthesis of New High-Temperature Geopolymers for Reinforced Plastics/Composites," *Proceedings of PACTEC '79, Society of Plastics Engineers*, Costa Mesa, California, USA, pp. 151-174, 1979. [Google Scholar]

[19] Nan Zhang et al., "Specimen Size Effects on the Mechanical Behaviors and Failure Patterns of the Mine Tailings-Based Geopolymer under Uniaxial Compression," *Construction and Building Materials*, vol. 281, 2021. [CrossRef] [Google Scholar] [Publisher Link]

[20] K. Poorveekan et al., "Investigation of the Engineering Properties of Cementless Stabilized Earth Blocks with Alkali-Activated Eggshell and Rice Husk Ash as a Binder," *Construction and Building Materials*, vol. 277, 2021. [CrossRef] [Google Scholar] [Publisher Link]

[21] H.K. Thejas, and Nabil Hossiney, "Compressed Unfired Blocks Made with Iron Ore Tailings and Slag," *Cogent Engineering*, vol. 9, no. 1, pp. 1-14, 2022. [CrossRef] [Google Scholar] [Publisher Link]

[22] Shaker M.A. Qaidi et al., "Recycling of Mine Tailings for the Geopolymers Production: A Systematic Review," *Case Studies in Construction Materials*, vol. 16, pp. 1-22, 2022. [CrossRef] [Google Scholar] [Publisher Link]

[23] Gregorio Palma et al., "Optimization of Geopolymers for Sustainable Management of Mine Tailings: Impact on Mechanical, Microstructural, and Toxicological Properties," *Minerals*, vol. 14, no. 10, pp. 1-22, 2024. [CrossRef] [Google Scholar] [Publisher Link]

[24] Pozhhan Mokhtari et al., "Valorization of Mine Tailings for Sustainable Geopolymer Production," *International Journal of Ceramic Engineering & Science*, vol. 7, no. 4, pp. 1-16, 2025. [CrossRef] [Google Scholar] [Publisher Link]

[25] Jorge Fernandes et al., "Life Cycle Analysis of Environmental Impacts of Earthen Materials in the Portuguese Context: Rammed Earth and Compressed Earth Blocks," *Journal of Cleaner Production*, vol. 241, 2019. [CrossRef] [Google Scholar] [Publisher Link]